



4-25-2019

Radiative double electron capture by ions in collisions with gas targets

Charles Taylor

Western Michigan University, charles.ja.taylor@outlook.com

Follow this and additional works at: https://scholarworks.wmich.edu/honors_theses

 Part of the [Physics Commons](#)

Recommended Citation

Taylor, Charles, "Radiative double electron capture by ions in collisions with gas targets" (2019). *Honors Theses*. 3177.
https://scholarworks.wmich.edu/honors_theses/3177

This Honors Thesis-Open Access is brought to you for free and open access by the Lee Honors College at ScholarWorks at WMU. It has been accepted for inclusion in Honors Theses by an authorized administrator of ScholarWorks at WMU. For more information, please contact maira.bundza@wmich.edu.



Double electron capture accompanied by single photon emission for ions colliding with gas targets

Lee Honors College Thesis

By: Charles J. Taylor

Committee Chair: Dr. John A. Tanis

Committee Member: Dr. A. Kayani

Collaborators: Dr. P. N S. Kumara (PhD student, graduated December 2018)

David S. La Mantia (PhD student)

Stephanie L. Buglione

Craig P. McCoy

Jacob S. White

Table of Contents

1. Introduction
 2. Process
 - 2.1 Electromagnetic Radiation
 - 2.2 Photoionization
 - 2.3 Double Photoionization
 - 2.4 REC
 - 2.5 RDEC
 3. History
 4. Kinematics
 - 4.1 REC Kinematics
 - 4.2 RDEC Kinematics
 5. Significance of gas targets vs. thin-foil solid targets
 6. Experimental Procedure
 7. Data Analysis/ Results
 - 7.1 Transitions
 - 7.2 X-ray gated TAC Spectra
 8. Cross Section
 9. Conclusion
- References

1. Introduction

In the 1600's Isaac Newton was among the first to describe the physical world mathematically. With this success came a belief of a clock-work universe. In other words, the belief that everything in the universe was 'wound-up', if one knew the position and momentum of a group of particles then one can calculate their behavior for all points in time [1]. When Newtonian mechanics was applied to things like atoms and electrons it did not work. In the 1900's quantum theory began to replace Newtonian mechanics (classical physics) in the realm of the very small, i.e., atoms, molecules and sub-atomic particles. Quantum theory suggested that it was impossible to predict the exact behavior of particles on an atomic level. The clock-work universe idea began to dissolve. After much work and effort by brilliant scientists it became apparent that the quantum world is much different than our perception of the world. One of the strangest things, as one zooms out from an atomic level, is all the 'quantum-ness' seems to disappear. In this document, one of the characteristics of the quantum world is investigated, electron-electron correlation, studied by the process of double electron capture accompanied with the simultaneous emission of a photon, otherwise known as radiative double electron capture (RDEC).

Scattering experiments are an important tool used in physics to understand the nature of matter at the fundamental level of molecules, atoms, and subatomic particles [2]. Studies involving how atoms interact with the electromagnetic spectrum offers a wide range of opportunities to understand the fundamental laws of nature. The study of RDEC offers unique insight into these rules for multielectron systems. More specifically, the method used in the present work for studying RDEC, using fully-stripped ions in collision with gas targets, where only two electrons are interacting without force from nearby electrons offers clear information into interpretation of electron-electron correlation [3]. RDEC can be considered the inverse of the fundamental process of double photoionization. Furthermore, RDEC promises to be one of the solutions for uncovering information needed for describing the wave function for two-electron systems in quantum mechanics. Other applications of RDEC studies include further insight into astrophysics, quantum theory, quantum electrodynamics and plasma physics.

2. Process

2.1 Electromagnetic Radiation

One of the most dramatic predictions in physics was in Maxwell's theory of electromagnetism. In 1865, he suggested that light existed as electromagnetic waves propagating at the speed of 3×10^8 m/s, i.e., the speed of light. The first successful observation of this proposal was performed by Heinrich Hertz in 1886 using a spark gap (cathode and an anode) that allowed light to pass through a quartz window to block ultraviolet light. Hertz noted, the spark gap was more intense if the quartz window was removed and ultraviolet light was used. This effect became known as the photoelectric effect. Albert Einstein successfully explained the theory of this effect, which won him a Nobel Prize in 1921. The photoelectric effect can be thought of as a specialized case of the more general effect known as photoionization, which occurs when a photon excites an atom to eject an electron, known as a photoelectron.

Light was misunderstood for most of human history. Today there are ample numbers of experiments to describe its properties and interactions. The smallest quantized bundle of light, a photon has negligible mass, and travels at a constant speed (the speed of light, $c = 3 \times 10^8$ m/s) with momentum equal to Planck's constant, h , divided by the wavelength, λ . A photon's speed is described by $c = \lambda f$, the wavelength times the frequency. Thus, a photon with a high frequency must have a small wavelength, or vice versa. The range of light that is visible to the human eye is very small compared to the entire detectable spectrum, which is categorized by wavelength. Visible light falls in the range of $\lambda \sim 10^{-7}$ m – 10^{-6} m. The smallest wavelength of our vision is blue light, and the largest wavelength is red light. Wavelengths smaller than blue light, which humans cannot see, are ultraviolet light with wavelengths $\lambda \sim 10^{-8}$ m, x-rays with $\lambda \sim 10^{-9}$ m, gamma rays with $\lambda \sim 10^{-12}$ m, and cosmic rays of $\lambda \sim 10^{-15}$. At the other end of the spectrum, with wavelengths larger than red light, and which cannot be seen by humans, are infrared light with $\lambda \sim 10^{-5}$ m, microwaves with $\lambda \sim 10^{-5}$ m, and radio waves of $\lambda \sim 1$ m. The energy of a photon is given by $E = hc/\lambda$. Therefore, if λ is small then the energy is large, and if λ is large then the energy is

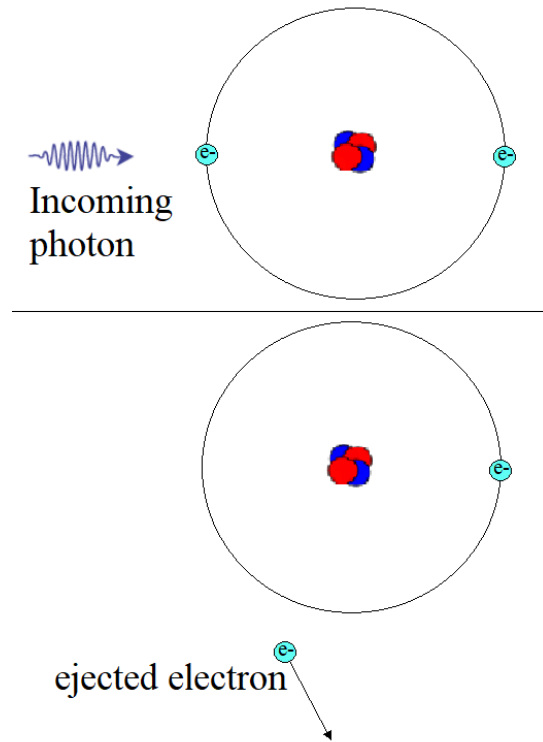
small. Processes in this work are concerned with photons in the x-ray range, which will be discussed in the kinematics section below.

It is worth recognizing here a simple and elegant law of nature known as the conservation of energy. An electron in an atom can interact with a photon and absorb some of its energy to transition to a higher energy state, while the remaining energy is conserved and emitted as a photon. The same happens in the inverse frame, i.e., an excited electron deexcites to a lower orbital and energy is conserved with the emission of a photon with energy equal to the transition energy. This concept will be useful in understanding the process of radiative electron capture (REC), where a single electron is captured accompanied by a simultaneous emission of a photon, and RDEC where two electrons are captured with the simultaneous emission of a photon.

2.2 Photoionization

Atoms have interesting interactions with electromagnetic radiation. It is known that a single photon can only interact with a single electron. So, if two electrons are affected by a single photon, it must be a quantum effect. For photoionization, an incoming photon can excite an atom to eject an electron, as shown in Figure 1. The collisional analog of photoionization is (REC) where an electron is captured to a projectile ion, and a photon is emitted. These two processes illustrate the point made earlier concerning photon-electron interactions.

Figure 2.2.1: Schematic showing the fundamental atomic process known as photoionization.

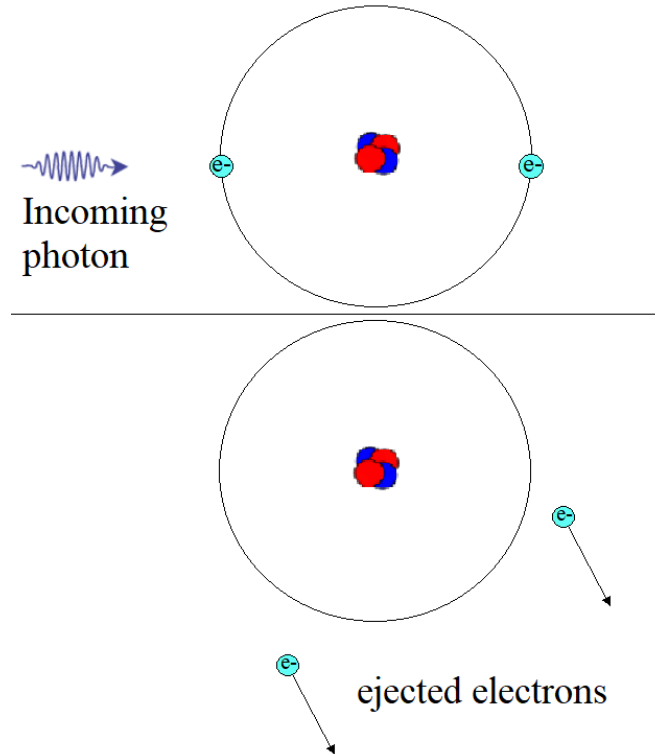


2.3 Double Photoionization

Cases concerning two electrons like double photoionization, where an incoming photon excites an atom to eject two electrons, are of interest due to the quantum effect between two electrons. The incoming photon dislodges an electron, while the electron-electron interaction causes an additional electron to be ejected from the atom, if the photon energy is enough to eject the two electrons, then energy is conserved. This process can be seen in Figure 2.3.1. RDEC can be considered the time inverse of double photoionization, where two electrons are captured from a target atom to the projectile ion and a single photon is emitted. These processes are of interest to this study because of the quantum effect between the electrons. The two electrons somehow “hold hands,” or in other words, they are correlated. So, electron correlation could be a deeper connection than stated earlier. The electromagnetic repulsion (or attraction) between two charged particles, caused by the Coulomb force, is well understood. However,

other unusual quantum properties have been identified. To understand this correlation more profoundly is the heart of the study of RDEC.

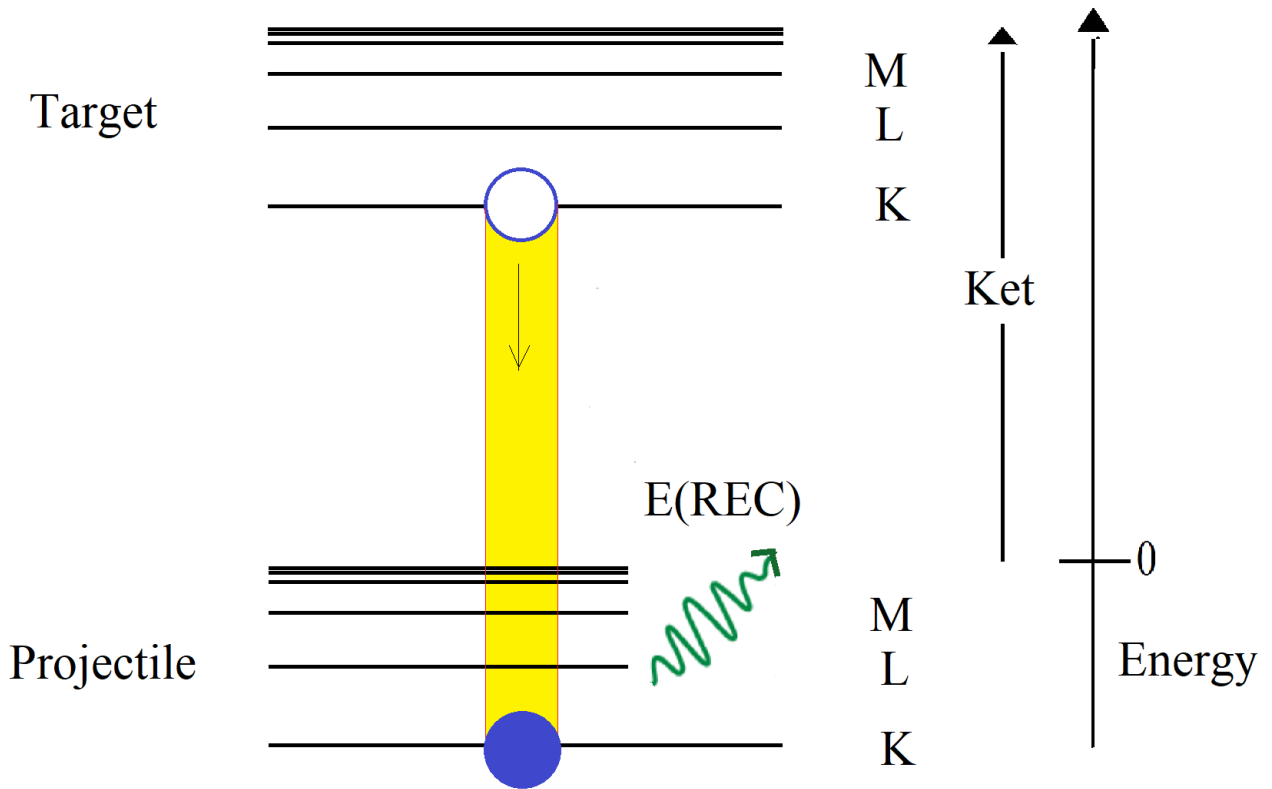
Figure 2.3.1: Schematic of the atomic process double photoionization



2.4 REC

Radiative electron capture (REC) is a single step quantum process that has been studied for nearly 50 years. REC occurs when a projectile ion captures an electron from a target atom with the simultaneous emission of a photon. REC is an important atomic process that can be used to study electron-photon interactions since it can be considered the time reverse process of photoionization. REC can also be considered the ion-atom collision analog of radiative recombination, in which a free electron is captured to the projectile ion and a photon is emitted. A depiction of REC from K shell to K shell is shown in Figure 2.4.1, where K_{et} is the kinetic energy of the target atom as seen from the rest frame of the projectile ion. The transition $K \rightarrow K$ was chosen to illustrate the process of REC in the figure although it is possible for other transitions to occur.

Figure 2.4.1: Schematic of the radiative electron capture (REC) process

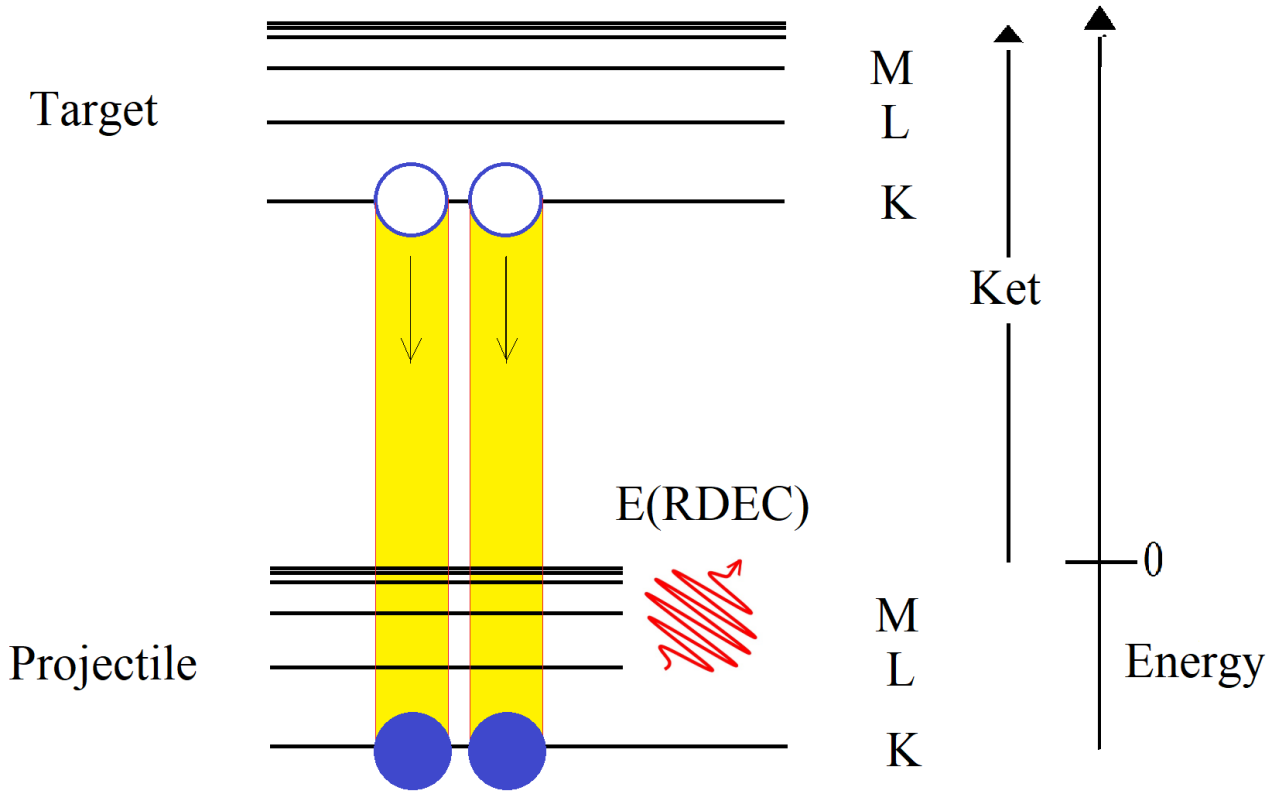


2.5 RDEC

Radiative double electron capture (RDEC) is a two-step quantum process that has been investigated experimentally since 1995. This process occurs when a projectile ion captures two electrons with the simultaneous emission of a single photon. Thus, RDEC can be considered the time reverse process of double photoionization. A depiction of RDEC from KK to KK is shown in Figure 2.5.1, where K_{et} is the kinetic energy of the target atom as seen from the rest frame of the projectile ion. It is possible for other transitions to occur, but these transitions are dependent on the charge state of the projectile and

will be discussed in the transition section. The transition, $KK \rightarrow KK$ was chosen to model the RDEC process in the figure.

Figure 2.5.1: Schematic of the radiative double electron capture (RDEC) process.



3. History

Radiative double electron capture was first theorized by Miraglia and Gravielle at the XVth International Conference on Photonic, Electronic and Atomic Collisions (ICPEAC), held in Brighton England in 1987 [5]. The first experimental study of RDEC for fully-ionized argon Ar^{18+} nuclei of energy to 11.4 MeV/u colliding with thin-foil carbon targets was reported in 1995 for results at the Gesellschaft

für Schwerionenforschung (GSI) accelerator facility in Darmstadt, Germany [6]. The units MeV/u are used to indicate the kinetic energy per atomic mass unit of the projectile ion, which is one million electron volts divided by the atomic mass of the projectile ion. In this experiment, thin carbon targets had thickness of 4-10 $\mu\text{g}/\text{cm}^2$. Carbon foils are widely used in collision experiments since they are simple to use and inexpensive to obtain. The units $\mu\text{g}/\text{cm}^2$ represents the areal density of the carbon foil, which is in micrograms (meaning $1 \times 10^{-6} \text{ g}$) divided by the area in centimeters squared (meaning $1 \times 10^{-2} \text{ m}$). For this work, RDEC was not observed, which was attributed to background events from electrons scattered inside the foil.

In 2003, the results of the next experimental study of RDEC were reported for fully-stripped uranium (U^{92+}) ions of relativistic energy 297 MeV/u colliding with an argon gas-jet target. In this work, there was no evidence of events corresponding to RDEC was found, a result that was likely due to insufficient counting times for the very thin (compared to carbon) target that was used.

In 2004 theoretical calculations [8] were published suggesting ways to improve the probability of observing RDEC. The first suggestion was to use beams of projectiles of lower energy compared to the higher energy work done previously. The second suggestion was to use projectiles of lighter to medium heaviness, e.g., nuclei in the range of about 2 to 35.

This motivated the work reported in 2010 at the tandem Van de Graaff accelerator facility at Western Michigan University (WMU) [9]. The experimental setup used a fully-stripped projectile beam of oxygen ions (O^{8+}) at 2.38 MeV/u energy. With oxygen having 8 protons in the nucleus, this was thought to be a good projectile since it matched the description of the suggestion from the theoretical paper [8]. The target used for this experiment was a thin carbon foil ($\sim 10 \mu\text{g}/\text{cm}^2$). For this work, RDEC counts were seen. A technique known as Rutherford backscattering was used to separately investigate the carbon target for impurities. This method is very precise and did not show evidence of impurities, indicating the first observation of RDEC.

A follow up experiment was done later at the WMU accelerator facility [10,11]. In this work a projectile beam of fluorine ions (F^{9+}) with energy of 2.21 MeV/u was used. The target was again a thin carbon foil. Similar results to the RDEC observation found in the previous experiment occurred, however, the RDEC counts could not be accurately determined. This time the carbon foil was found to contain several contaminations using the same proton beam test described above. The contaminations found contributed to x-ray events in the RDEC region. Therefore, an estimate for the probability of RDEC from this experiment was difficult to determine.

A final experiment done at GSI in 2013 was reported [12]. Here, a projectile beam of Cr^{24+} at 30 MeV/u collided with helium and nitrogen jet targets. No x-ray events corresponding to the RDEC energy region were seen. However, this experiment took data only for a short amount of time and the negative results were likely due to the insufficient counting times.

To summarize the history, the GSI experiments [6,7,12] did not show any experimental evidence for the RDEC process. The two experiments done at WMU [9,11] and the present thesis document covering the experiment done during the summer of 2018 at the WMU accelerator facility, showed experimental evidence for RDEC.

4. Kinematics

4.1 REC Kinematics

Radiative electron capture (REC) is a well-known ion-atom collision process where one target electron is captured to the projectile ion while simultaneously emitting a photon in the x-ray spectrum. The energy of the photon can be derived non-relativistically in the projectile reference frame by considering the conservation of energy mentioned above. Before the collision the electron in the target has an intrinsic momentum \vec{p}_{it} , and a potential energy V_{it} from its orbit around its nucleus. In the projectile frame of reference, the target appears to be in motion while the projectile is at rest and therefore

the target electron has a momentum $\vec{\rho}_0$ from the kinetic energy of the projectile in the lab frame. The total energy is defined by the kinetic energy added to the potential energy. The initial energy of the target electron is thus,

$$\begin{aligned}
 E_i &= \frac{1}{2m_e} (\vec{\rho}_0 + \vec{\rho}_{it})^2 + V_{it} = \frac{1}{2m_e} (\rho_0^2 + 2\vec{\rho}_0 \cdot \vec{\rho}_{it} + \rho_{it}^2) + V_{it} \\
 &= K_{et} + \frac{1}{m_e} (\vec{\rho}_0 \cdot \vec{\rho}_{it}) + B_t = K_{et} + B_t + \frac{1}{m_e} (\rho_0 \rho_{it} \cos\theta) = K_{et} + B_t + \frac{1}{m_e} (m_e v_0 \rho_{it} \cos\theta) \\
 &= K_{et} + B_t + \vec{v}_p \cdot \vec{\rho}_{it}
 \end{aligned}$$

In the collision, the electron from the target is captured to the projectile and a photon is emitted. Once captured the electron will have an intrinsic momentum to the projectile nucleus $\vec{\rho}_{ip}$ and a potential energy V_{fp} due to the orbit around the projectile nucleus. The emitted photon will have energy E_{REC} . Thus, the final energy will look like

$$E_f = \frac{1}{2m_e} (\vec{\rho}_{ip})^2 + V_{fp} + E_{REC} = B_p + E_{REC}$$

The conservation of energy states that there is no change between the final energy and the initial energy. Mathematically this says

$$E_f - E_i = 0.$$

Substituting in the values for E_f and E_i ,

$$(B_p + E_{REC}) - (K_{et} + B_t + \vec{v}_p \cdot \vec{\rho}_{it}) = 0$$

and solving for E_{REC}

$$E_{REC} = K_{et} + B_t - B_p + \vec{v}_p \cdot \vec{\rho}_{it}$$

The term K_{et} is the kinetic energy of the target electron as seen from the projectile rest frame. The binding energies of the captured electron from the target to the projectile are denoted by B_t and B_p , where these quantities are negative by convention. The dot product is the velocity of the projectile \vec{v}_p and the momentum of the bound electron \vec{p}_{it} , which give the energy of the bound electron on the path of the projectile. This term, $\vec{v}_p \cdot \vec{p}_{it}$, is known as the Compton profile [14] and it broadens the range of the x-rays associated with this process. Therefore, the center of the peak formed can be found using the first three terms, and the fourth term broadens the peak structure.

4.2 RDEC Kinematics

Radiative double electron capture (RDEC) is a two-electron collision process between the incoming ion and the target, in which the ion captures two electrons from the target with the simultaneous emission of a photon. The energy of the photon can be described mathematically the same as REC except there are two electrons, therefore two of every term. The RDEC energy expression for the photon looks like

$$E_{RDEC} = 2K_{et} + B_t^{(1)} + B_t^{(2)} - B_p^{(1)} - B_p^{(2)} + \vec{v}_p \cdot \vec{p}_{it}^{(1)} + \vec{v}_p \cdot \vec{p}_{it}^{(2)}.$$

The term $2K_{et}$ represents the kinetic energy of the two electrons in the target atom as seen from the projectile frame of reference. The binding energies of the two electrons captured from the target are $B_t^{(1)}$ and $B_t^{(2)}$ and those of the projectile ion are $B_p^{(1)}$ and $B_p^{(2)}$; by convention these quantities are negative. The dot products are the velocities of the projectile as seen by the two electrons $\vec{v}_p^{(1)}$ and $\vec{v}_p^{(2)}$ and the intrinsic momenta of the bound electrons are $\vec{p}_{it}^{(1)}$ and $\vec{p}_{it}^{(2)}$, which give the contribution to the energy of each bound electron on the path of the projectile. The terms $\vec{v}_p \cdot \vec{p}_{it}^{(1)}$ and $\vec{v}_p \cdot \vec{p}_{it}^{(2)}$ are again known as the Compton profile, and it broadens the range of the x-rays associated with this process.

Therefore, the center of the peak formation can be found using the terms before the dot products, and the dot products broaden the peak structure.

5. Significance of gas targets vs. thin-foil solid targets

The previous experiments done at WMU used a carbon foil target. With carbon foil as a target there is a high probability for multi-collisions to occur, i.e., the projectile can interact with more than one atom in the carbon foil. The solid target is also more likely to be contaminated with other elements resulting in counts in the spectra not associated with REC or RDEC. Therefore, a gas target is preferred for the RDEC experiment.

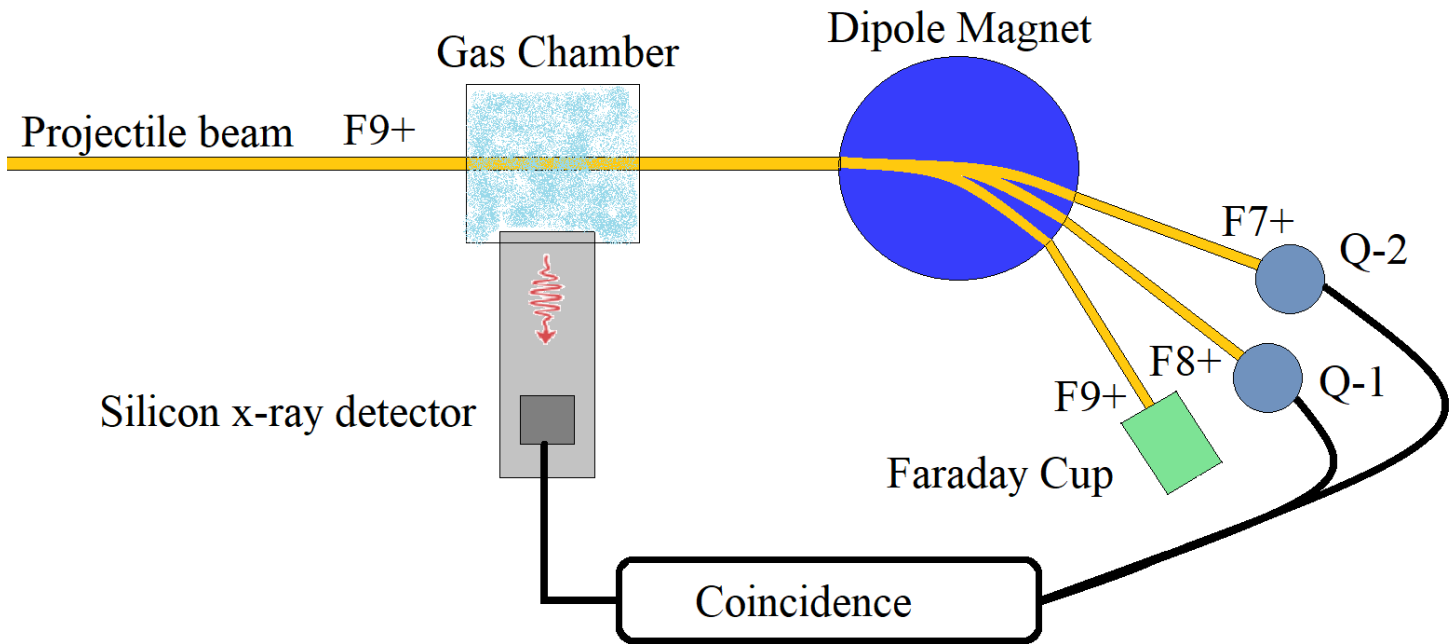
The first benefit of using a gas target is the avoidance of multi-collisions. With gas targets, the pressure can be controlled and, therefore, the number of single collisions per projectile, can be easily set. The other benefit is the purity of the target. With high purity gases the experiment can be run without counts coming from contaminants.

6. Experimental Procedure

A beam of atomic particles can be fully stripped of all its electrons, leaving just the bare nucleus, which consists of tightly packed positively charged protons and neutrons with no charge. For example, in this experiment a beam of fluorine atoms was stripped of all its electrons, or just one was left on the ion, leaving the fluorine nucleus with a charge state of $9+$ or $8+$. Ionized particles tend to capture electrons. The positive nucleus attracts negatively charged electrons via the electromagnetic force, and thus processes like REC and RDEC can occur. The beam of bare and nearly bare fluorine ions is obtained from the tandem Van de Graaff accelerator at WMU with a high voltage put on the machine.

For the present experiment 2.11 MeV/u beams of F^{9+} and F^{8+} collided with a N_2 gas target at 8 mTorr (milliTorr). The beam was obtained from the tandem Van de Graaff accelerator at WMU as discussed above. X-ray events that occurred were observed using a solid-state silicon detector positioned at 90 degrees to the gas chamber. Some of the ions passing through the target capture electrons undergoing REC or RDEC. A dipole magnet was used to separate the different emerging charge states onto corresponding particle detectors associated with double charge exchange (Q-2) and single charge exchange (Q-1). The projectiles with no charge exchange struck the end of the beam line and were collected by a Faraday cup. When the x-ray detector or the particle detectors receive signals, electronics devices are used to process the signals. Coincidences between the x rays observed and the particles striking the (Q-2) and (Q-1) detectors are studied using time-to-amplitude converters (TACs). When an x ray is detected a timer is started. The timer is stopped when the particle associated with the emitted x ray strikes a particle detector. Information from the coincidence timing is fed into an analog-to-digital converter (ADC), where it is converted to a number that is saved by a computer. The software stores this number into a bin. Over time events accumulate in the bins and peaks begin to form in the spectra associated with Q-1 and Q-2 particle detectors. These events thus allow for particles to be matched to their corresponding x rays. The kinematic equations derived above are used to calculate the regions of interest in the graphs, and events corresponding to RDEC can be identified and analyzed. A view of the experimental apparatus can be seen in Figure 6.1.1.

Figure 6.1.1: Schematic diagram of the experimental apparatus.



7. Data Analysis/ Results

7.1 Transitions

In the summer of 2018, at the tandem Van de Graaff accelerator facility at WMU, an attempt to observe RDEC was made. In this experiment a 2.11 MeV/u F^{9+} ion beam was incident on a gaseous molecular nitrogen target. The REC and RDEC events correspond to photons of energies based on the kinematics described above. The calculated peaks of REC and RDEC for different transitions in F^{9+} on nitrogen collisions are shown in Table 1 below.

Table 1. Calculated peak energies of REC and RDEC for 2.11 MeV/u $F^{9+} + N_2$ collisions [2]

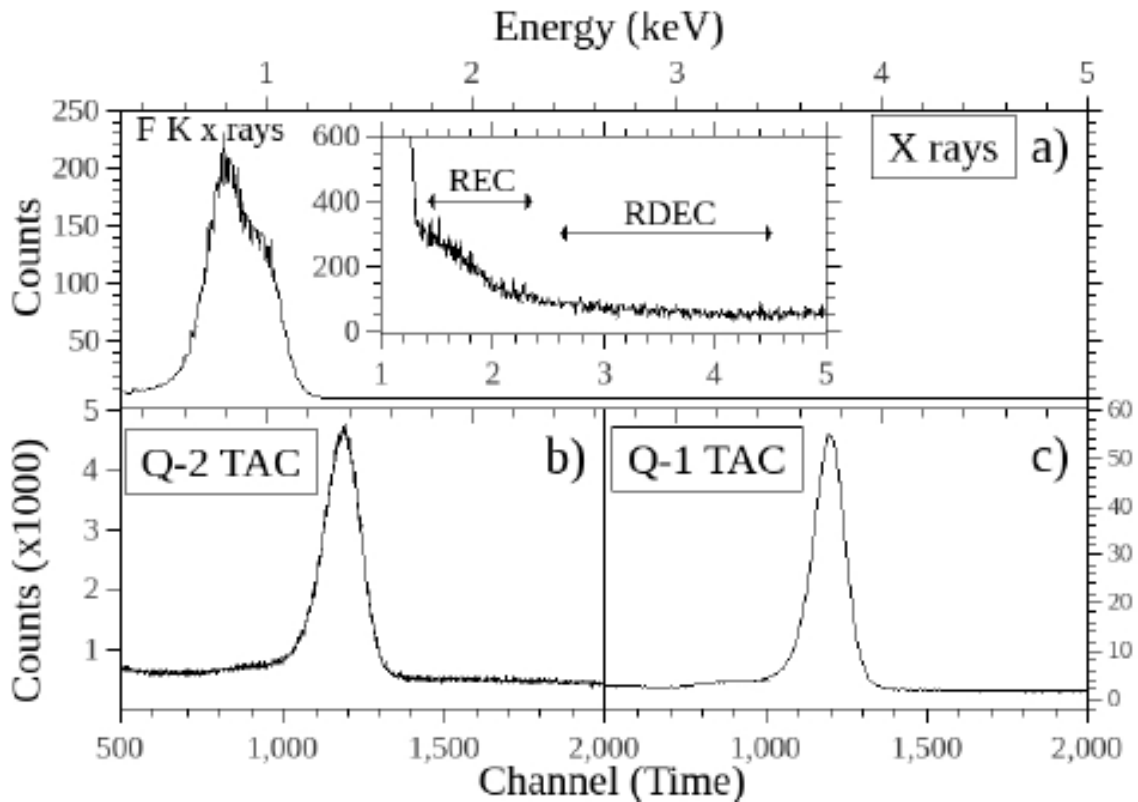
	<i>Transition</i>	<i>Peak Energy (keV)</i>
<i>REC</i>	$K \rightarrow L$	0.96
	$V \rightarrow L$	1.37
	$K \rightarrow K$	1.85
	$V \rightarrow K$	2.25
<i>RDEC</i>	$KK \rightarrow KL$	2.81
	$VK \rightarrow KL$	3.16
	$KK \rightarrow KK$	3.55
	$VV \rightarrow KL$	3.62
	$VK \rightarrow KK$	3.91
	$VV \rightarrow KK$	4.31

The symbols on the left of the arrow represent the electron(s) in their initial shell(s) of the target atom. The symbols to the right of the arrow represent the electrons in their final shells. The electrons that begin in different shells are expected to have low electron correlation. Therefore, transitions like $VK \rightarrow KL$ or $VK \rightarrow KK$ (V represents the valence shell of the atom and K is the inner-most shell of the atom) have the least electron correlation and are expected to contribute the least to events corresponding to RDEC [2]. However, electrons in the same shell have a higher electron correlation. Therefore, transitions that start with electrons in initial positions such as VV and KK are expected to contribute more to events corresponding to RDEC. For the fluorine 8+ projectile beam there is already one electron in the K shell. So, there is only one vacant position in the K shell, which means that events that contribute to RDEC result in final shells like KL. Therefore, for the fluorine 8+ projectiles RDEC transitions $KK \rightarrow KK$, $VV \rightarrow KK$, and $VK \rightarrow KK$ are not allowed. Also, the fluorine 9+ has a higher charge state and therefore is expected to have a stronger electromagnetic attraction for the electrons than the fluorine 8+ projectiles.

7.2 TAC and X-ray Spectra

The coincidences between the x-ray being detected and the corresponding particle reaching its detector Q-1 or Q-2 are studied using the time-to-amplitude converters (TACs). The time between these two events is converted to an amplitude, with a longer time, giving a larger amplitude. This information is then sent to an analog-to-digital (ADC) converter, which gives the computer a number and the software stores this number in a bin as an event. Overtime these events build up in the bins and peak structures form. TAC spectra associated with single charge exchange Q-1 and double charge exchange Q-2 particle detectors are the result and are shown in Figure 7.1.1, along with the entire x-ray spectra. The large peak in the x-ray spectrum seen in the figure below corresponds to fluorine K alpha x rays (large peak), and the much smaller peaks to REC and RDEC (zoomed in graph).

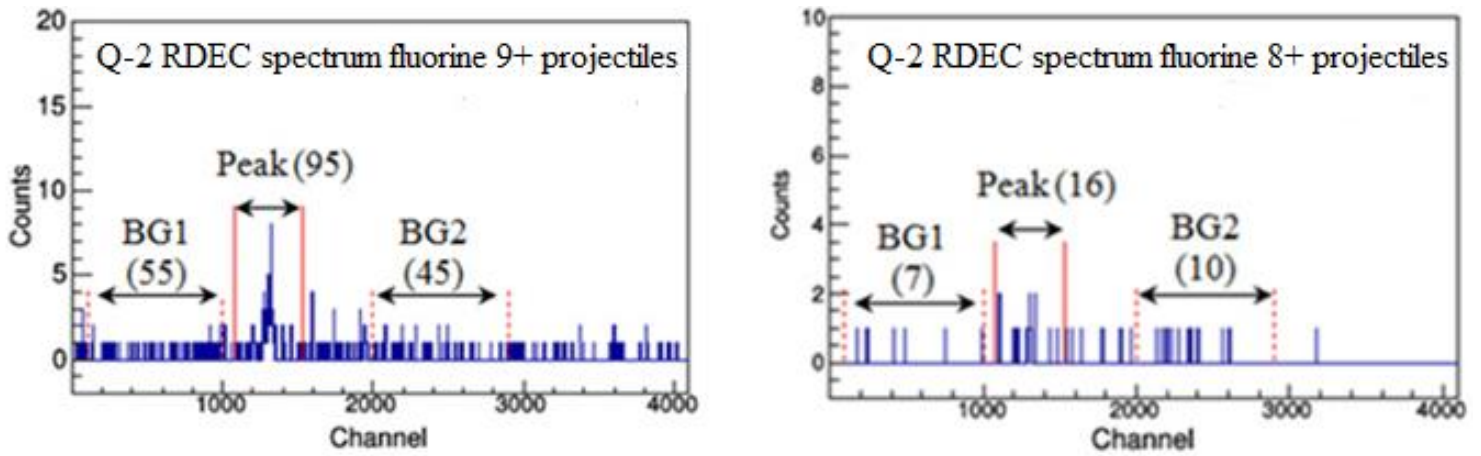
Figure 7.1.1 X-ray energy spectrum and Q-1 and Q-2 TAC spectra for 2.11 MeV/u $F^{9+} + N_2$



7.2 X-ray gated TAC spectra

Here, the x-ray spectrum was gated in the region of the RDEC events (from ~2.8 – 4.3 keV from Table 1). The computer was then asked to retrieve the TAC events that correspond to the x rays within the gate. This is known as an x-ray gated TAC spectrum, which allows for counts from RDEC to be identified. The x-ray gated TAC spectra for F^{9+} and F^{8+} are shown in Figure 7.2.1.

Figure 7.2.1 X-ray gated Q-2 TAC spectra for F^{9+} and F^{8+} projectiles. BG1 and BG2 are background regions. The numbers in parenthesis represent the number of counts in each region.



To find the actual number of RDEC counts the background counts are subtracted using the following formula.

$$\begin{aligned}
 (\text{Total events in region}) - \frac{(\text{Total number of background counts})}{(\# \text{ of bins in the region})} \cdot (\# \text{ of bins in the region}) &= \\
 &= (\text{RDEC events in region})
 \end{aligned}$$

The RDEC events within the regions of the Q-2 spectra for F^{9+} and F^{8+} beams were calculated to be 70 and 12, respectively.

8. Cross Section

The term cross section is used to define the probability that two particles will collide and interact via the processes of interest. The probability that they will collide is proportional to the “sizes” of the particles. In the current experiment the RDEC differential cross section at 90 degrees was measured and from this the total cross section was inferred to compare it with the calculated one from theory. Cross sections are independent of the intensity and focus of the ion beam; therefore, cross section measurements made at the WMU accelerator facility can be compared to the cross sections found by other researchers.

In the present experiment a nitrogen gas target was used. Once a projectile ion enters the gas chamber and before it exits, a collision with a nitrogen molecule can take place at any time while the projectile is inside the gas cell. The detector was located 90 degrees to the gas chamber. Then the differential cross section for the process is calculated from

$$\frac{d\sigma}{d\Omega} = \frac{N_{event}}{N_{beam}} \frac{1}{\epsilon_x \Delta\Omega (NLP)},$$

where N_{beam} is the total number of incident particles and N_{event} is the number of events observed. The term (NLP) is the thickness of the gas target in molecules/cm², where N is the number of molecules in the target gas per unit volume per unit pressure 3.3×10^{13} molecules · cm⁻³ · mTorr⁻¹ [15], L (in cm) and P (in mTorr) are the length of the gas cell and the pressure of the gas target. The solid angle term $\Delta\Omega$ was equal to value for 90 degrees expressed in steradian⁻¹. The efficiency of the detector is ϵ_x and for the present experiment it was about 1.

REC emission for the x rays has a $\sin^2\theta$ angular dependency [12] and this is assumed to be the same for RDEC. Therefore, the total cross sections for both REC and RDEC are calculated from

$$\sigma_{total} = \int_0^\pi \int_0^{2\pi} \left(\left(\frac{d\sigma}{d\Omega} \right)_{\theta=90^\circ} \sin^2\theta \right) \sin\theta d\theta d\varphi = \frac{8\pi}{3} \left(\frac{d\sigma}{d\Omega} \right)_{\theta=90^\circ}$$

In this experiment, only the differential RDEC and REC cross sections were measured. The total RDEC cross sections for this work were calculated using the formula above for fluorine 9+ and 8+ ions and can be seen in Table 2 below. Theoretical calculations for the present work have not yet been performed.

Table 2. Differential (at 90 degrees) and total RDEC cross sections for 2.11 MeV/u F⁹⁺ + N₂ [4]

<i>Projectile</i>	<i>Target</i>	<i>Differential RDEC cross section at 90 degrees (10⁻²⁴ cm²/atom/sr)</i>	<i>Total RDEC cross section (10⁻²⁴ cm²/atom)</i>
2.11 MeV/u F ⁹⁺	N ₂	0.30 ± 0.17	2.5 ± 1.4
2.11 MeV/u F ⁸⁺	N ₂	0.05 ± 0.03	0.42 ± 0.25

9. Conclusion

For this thesis document, I participated in the 2018 summer experiment using 2.11 MeV/u F⁹⁺ and F⁸⁺ beams incident on a nitrogen gas target to observe RDEC. The goal for this project was to investigate the atomic process of RDEC. A gas target was chosen to avoid multi-collision effects that were seen in past experiments with a carbon foil. The RDEC process was observed for both fully-ionized F⁹⁺ and one electron F⁸⁺ projectiles in collisions with nitrogen. In this experiment, the total RDEC cross section for F⁹⁺ + N₂ is about 2.5 (10⁻²⁴ cm²/atom) and for F⁸⁺ + N₂ it is about 0.42 (10⁻²⁴ cm²/atom). Therefore,

the cross section for F^{9+} is greater than the one for F^{8+} by about a factor of 6. In the previous experiment performed at WMU with a projectile beam of O^{8+} in collision with a thin-foil carbon target [9], an RDEC total cross section of about $5.5 (10^{-24} \text{ cm}^2/\text{atom})$ was reported. The previous results for a 2.21 MeV/u F^{9+} projectile beam in collision with a thin-foil carbon target, gave an RDEC total cross section of about $9.1 (10^{-24} \text{ cm}^2/\text{atom})$ [11]. So, experiments [9,11] compared to this current work for F^{9+} projectiles on gas targets were larger by factors of roughly 2 and 4, respectively.

References

- [1] V3. Advanced lab manual. Chaos Lab.
- [2] N. S. Kumara, Ph. D dissertation at WMU in 2019. *Radiative Double Electron Capture (RDEC) By Fully-Stripped Fluorine Ions in Collisions with Nitrogen*.
- [3] D. S. La Mantia, P. N. S. Kumara, S. L. Buglione, C. P. McCoy, C. J. Taylor, J. S. White, A. Kayani, and J. A. Tanis. *Radiative Double Electron Capture for 2.11 MeV/u $F^{9-8=} + N_2$, Ne*. Submitted to Phys Rev Lett 2019.
- [4] P.N.S. Kumara, D. S. La Mantia, S. L. Buglione, C. P. McCoy, C. J. Taylor, J. S. White, A. Kayani, and J. A. Tanis. *Observation of Radiative Double Electron Capture (RDEC) For $F^{9+} + N_2$* . Accepted by X-ray Spectrometry 2019.
- [5] J. E. Miraglia and M. S. Gravielle, *XVth International Conference on Photonic, Electronic and Atomic Collisions, Brighton, UK, July 1987, Book of Abstracts*. p. 517.
- [6] A. Warczak, M. Kucharski, Z. Stachura, H. Geissel, H. Irnich, T. Kandler, C. Kozhuharov, P.H. Mokler, G. Münzenberg, F. Nickel, C. Scheidenberger, Th. Stöhlker, T. Suzuki and P. Rymuza, *Radiative double electron capture in heavy-ion atom collisions* Nucl. Instrum. Methods Phys. Res. B **98**, 303 (1995).
- [7] G. Bednarz, D. Sierpowski, Th. Stöhlker, A. Warczak, H. Beyer, F. Bosch, A. Bräuning-Demian, H. Bräuning, X. Cai, A. Gumberidze, S. Hagmann, C. Kozhuharov, D. Liesen, X. Ma, P.H. Mokler, A. Muthig, Z. Stachura and S. Toleikis, *Double-electron capture in relativistic U^{92+} collisions at the ESR gas-jet target*. Nucl. Instrum. Methods Phys. Res. B **205**, 573 (2003).
- [8] A. I. Mikhailov, I. A. Mikhailov, A. V. Nefiodov, G. Plunien and G. Soff, *Correlated double-electron capture with emission of a single photon*. Phys. Lett. A **328**, 350 (2004).
- [9] A. Simon, A. Warczak, T. Elkafrawy and J. A. Tanis, *Radiative Double Electron Capture in Collisions of O^{8+} Ions with Carbon*. Phys. Rev. Lett. **104**, 123001 (2010).
- [10] T. Elkafrawy, A. Warczak, A. Simon and J. A. Tanis, *Evidence for Radiative Double Electron Capture (RDEC) in F^{9+} On Carbon Collisions*. AIP Conf. Proc. **1525**, 64 (2013).
- [11] T. Elkafrawy, A. Simon, J. A. Tanis, and A. Warczak, *Single-photon emission associated with double electron capture $F^{9+} + C$ collisions*. Phys. Rev. A **94**, 042705 (2016).
- [12] N. Winters, A. Warczak, J. A. Tanis, T. Gassner, A. Gumberidze, C. Kozhuharov, S. Hagmann, P.M. Hillenbrand, N. Petridis, R. Reuschl, M. Schwemlein, R. Strzalka, D. Sierpowski, U. Spillmann, S. Trotsenko, G. Weber, D. F. A Winters, Z. Yin and Th. Stöhlker, *A study of radiative double electron capture in bare chromium ions at the ESR*. Phys. Scr.T **156** 014048 (2013).
- [13] E. A. Mistonova and O. Yu. Andreev, *Calculation of the cross section of radiative double-electron capture by a bare nucleus with emission of one photon*. Phys. Rev. A **87**, 034702 (2013).
- [14] Biggs F., Mendelson, L. B., and Mann, J. B., *Hartree-Fock Compton profiles for the elements*. Atomic Data and Nuclear Data Tables **16** 201 (1975).

[15] Haynes, M. William. Handbook of Chemistry and Physics. Edition 84, Published by Taylor & Francis, (2004).